Inference of Cultural Transmission Modes Based on Incomplete Information

Bryan Wilder[1] *and Anne Kandler*[2,3]*

ABSTRACT

In this article we explore the theoretical limits of the inference of cultural transmission modes based on sparse population-level data. We approach this problem by investigating whether different transmission modes produce different temporal dynamics of cultural change. In particular, we explore whether different transmission modes result in sufficiently different distributions of the average time a variant stays the most common variant in the population, t_{max}, so that their inference can be guaranteed on the basis of an estimate of t_{max}. We assume time series data detailing the frequencies of different variants of a cultural trait in a population at different points in time and investigate the temporal resolution (i.e., the length of the time series and the distance between consecutive time points) that is needed to ensure distinguishability between transmission modes. We find that under complete information most transmission modes can be distinguished on the basis of the statistic t_{max}; however, we should not expect the same results if only infrequent information about the most common cultural variant in the population is available.

The question of how ideas, knowledge, or even behaviors are transmitted between different individuals of a population has sparked an enormous amount of theoretical and empirical research in the last decade (e.g., Baum et al. 2004; Bentley et al. 2004; Henrich 2001; Mesoudi and O'Brien 2008; Rendell et al. 2010, 2011). Naturally, fine-grained individual-level data detailing who learns from whom would be most suited to answer these questions empirically. However, outside experimental conditions, large individual data sets of this kind are difficult to obtain, especially in premodern contexts. Studies such as those of Beheim et al. (2014), who used historical records of the board game Go, and Henrich and Broesch (2011), who used contemporary data from Fiji to determine the relative importance of different cultural transmission processes, are remarkable exceptions.

Often, population-level data describing the frequencies of different cultural variants in a population at different points in time are the only information researchers have about the process of cultural transmission (Shennan 2011). But the assumption that temporal changes in the frequencies of cultural variants over time reflect the dynamic of the underlying cultural transmission process (Boyd and Richerson 1985; Cavalli-Sforza and Feldman 1981) leads naturally to the question of how accurately those transmission modes can be inferred from potentially sparse, population-level data. Recently, researchers have started exploring the effects of time averaging on the accuracy of identifying cultural transmission

[1]University of Central Florida, Orlando, Florida.
[2]City University London, London, United Kingdom.
[3]Santa Fe Institute, Santa Fe, New Mexico.

*Correspondence to: Anne Kandler, City University London, London ECIV 0HB, UK. E-mail: anne.kandler.1@city.ac.uk.

KEY WORDS: CULTURAL TRANSMISSION, STATISTICAL INFERENCE, SAMPLING SCHEME.

Human Biology, Summer 2015, v. 87, no. 3, pp. 193–204.

modes, in particular on the accuracy of identifying neutral evolution (Madsen 2012; Premo 2014; Porčić 2014). Time averaging is defined as a phenomenon "whereby cultural remains deposited at different times come to be preserved together and thus appear to be pene-contemporaneous" (Premo 2014; Kidwell and Behrensmeyer 1993; Kowalewski 1996), and it has been shown that it diminishes our ability to correctly detect patterns of neutral evolution in population-level data (Premo 2014). Further, Eerkens et al. (2005) investigated the relationship between phylogenetic signature in population-level data and cultural transmission modes and concluded that some transmission modes maintain phylogenetic signature better than others.

In this article, we contribute to the discussion of how well cultural transmission modes can be inferred from population-level data by exploring the theoretical limits of such a statistical inference procedure. We base our considerations on time series data detailing the frequencies of different variants of a cultural trait in a population at different points in time and approach the inference problem by investigating whether different transmission modes result in different values of certain population-level statistics. If this is the case, then transmission modes are distinguishable, and observed estimates of those statistics are informative about the underlying transmission mode.Conversely, if transmission modes are not distinguishable (or only partially distinguishable), then different transmission modes may result in similar values of population-level statistics. Consequently, observed estimates of those statistics could have been produced by a number of cultural transmission modes (Cavalli-Sforza and Feldman 1981).

In Kandler et al. (2015) we developed a simulation framework that tracks the temporal changes in frequency of different variants of a cultural trait under the assumptions that cultural transmission occurs in a vertical, horizontal, oblique, or unbiased way (see, e.g., Cavalli-Sforza and Feldman 1981):

a. *Vertical transmission* describes the transmission from parents to offspring.
b. *Horizontal transmission* describes the transmission between (related or unrelated) individuals of the same age group.
c. *Oblique transmission* describes the transmission from individuals of one age group to individuals of younger age groups who are not their direct descendants.
d. *Unbiased transmission* describes the transmission between all individuals of the population.

Importantly, the framework produces frequency data, similar to observable ones, conditioned on the considered transmission modes. This enables us to ask the following question: given the generated frequency data, how well can we theoretically infer the (known) underlying cultural transmission mode? In Kandler et al. (2015) we found that the frequency distribution of the cultural variants in the population at a single point in time does not carry a strong enough signature about the transmission process. That is, we cannot reliably distinguish between transmission modes on the basis of, for example, the level of cultural diversity in the population.

However, the temporal dynamic of cultural change possesses more information. In situations of high rates of cultural transmission, we can distinguish between vertical and horizontal transmission, vertical and unbiased transmission, unbiased and oblique transmission, and horizontal and oblique transmission on the basis of the average time the most common variant remains the most frequent in the population. But crucially, this result relies on the fact that we have information about the most common variant at every point in time, which is, especially for historical case studies, very rarely the case. So what is the minimum temporal resolution of the data that is needed to guarantee these distinguishability results?

We note that cultural transmission can occur in many more ways than the four transmission modes considered here (see, e.g., Boyd and Richerson 1985; Laland 2004; Morgan et al. 2012), but the aim of the study is to explore the data resolution that is needed to obtain distinguishability results close to the theoretically possible results.

In the following we briefly summarize the simulation framework and the statistical inference procedure developed in Kandler et al. (2015). We then assume that we have information only about the most frequent variant at a certain number of points in time and analyze how incomplete

(temporal) information influences the power of the inference procedure. This analysis also allows us to give suggestions about the minimum time resolution of the sample that is needed to guarantee theoretical distinguishability between the cultural transmission modes considered in this study.

The Model

We consider a population of N individuals where each individual is characterized by a set of four discrete cultural traits. Those traits can take five different variants, and we assume that the traits differ only in the way they are transmitted. In the following,

- v stands for traits that are transmitted vertically;
- h stands for traits that are initially transmitted vertically and horizontally during an individual's lifetime;
- o stands for traits that are initially transmitted vertically and obliquely during an individual's lifetime; and
- u stands for traits that are initially transmitted vertically and in an unbiased way during an individual's lifetime.

We further assume that offspring inherit all cultural traits from their parents but may have the opportunity for cultural transmission during their lifetime. At each point in time an individual i is described by the variables I_x^i, with $x \in \{v, h, o, u\}$ summarizing individual i's acquired variants. It holds $I_x^i \in \{1, \ldots, 5\}$ for $x = v, h, o, u$. Further, we define five age groups covering ages 0–10, 11–20, 21–30, 31–40, and 41–50, respectively, and the variable I_{age}^i denotes individual i's age group. At each time step (which is equal to 10 years), all individuals are subject to a number of demographic and cultural processes (as detailed below), resulting in frequency changes of the five variants of the cultural traits in the population.

Demographic Processes

At each time step, individuals age and have a chance of reproducing and dying. Aging means that individuals move to the next age group. We assume the maximum age to be 50; consequently, all individuals moving to age group 6 die with probability 1. Additionally, individuals can die with probability P_{death} in each time step. We further assume a constant population size $N = 100$. Therefore, the number of individuals entering the population is given by the difference between N and the number of deaths in the considered time step. Reproduction occurs asexually; an individual of age group 2 or 3 is chosen at random and produces an offspring that inherits its trait values. However, with a small probability μ a mutation occurs and the offspring inherits a trait value different from the parent's. This process of reproduction is repeated until the population size N is reached. Together these demographic processes produce a pyramid-shaped age structure with fewer individuals in older generations. It is possible that all potential parents die before reproducing, resulting in the extinction of the population. The results shown in this article, however, are based on simulation runs where the population survived for the entire duration of the simulation.

Cultural Processes

Individuals acquire and change their cultural make-up through the process of cultural transmission. In the case of vertical transmission individual i inherits the cultural variant from its parent with probability $1 - \mu$, whereas with probability μ a mutation occurs and individual i acquires a variant randomly selected from the remaining four alternatives. Vertically transmitted traits do not change during an individual's lifetime. We stress that all traits are initially transmitted vertically; however, in the case of horizontal, oblique, and unbiased transmission, an individual engages with probability P_{within} in interactions with other individuals of the population in each time step and potentially changes the values of the traits h, o, and u. In detail, if transmission occurs horizontally, individual i randomly chooses another individual j from its own age group and with probability $1 - \mu$ adopts individual j's cultural variant

$$I_h^i = I_h^j \text{ with } I_{\text{age}}^i = I_{\text{age}}^j. \tag{1}$$

If transmission occurs obliquely, individual i randomly chooses another individual j from an older age group and with probability $1 - \mu$ adopts individual j's cultural variant

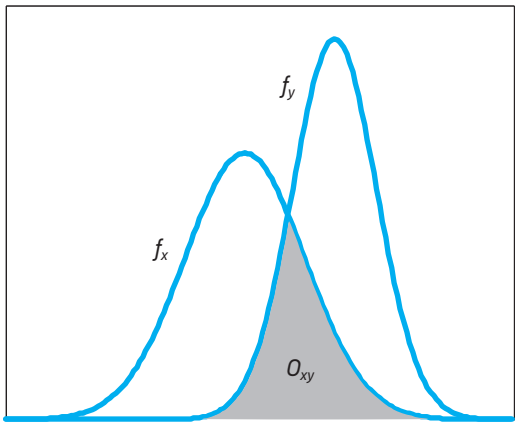

FIGURE 1. Area of overlap O_{xy}.

$$I_o^i = I_o^j \text{ with } I_{\text{age}}^i < I_{\text{age}}^j . \quad (2)$$

If transmission occurs in an unbiased manner, individual i randomly chooses another individual j from the entire population regardless of age group and with probability $1 - \mu$ adopts individual j's cultural variant

$$I_u^i = I_u^j . \quad (3)$$

In all transmission events, mutations occur with probability μ. In this case an individual adopts a randomly selected variant. Consequently, together with the interaction probability P_{within}, the mutation rate μ controls the rate of change in the population: the higher the probabilities P_{within} and μ, the more the cultural composition of the population can change in every time step.

The simulation framework tracks the frequencies of the different variants of the cultural traits v, h, o, and u in the population at every point in time. To describe the temporal dynamic of cultural change, we determined the average time a variant stays the most common variant in the population, denoted by $t_{\max}$. This statistic is a measure for quantifying the speed of cultural change. Bentley et al. (2007; further analyzed by Evans and Giometto 2011) described the temporal dynamic using turnover rates (defined as the number of new variants that enter the list of the l variants with the highest frequency in the population). However, due to our restriction to five possible cultural variants, turnover rates cannot be meaningfully applied to our situation. Additionally, the $t_{\max}$ statistic requires "only" knowledge of the cultural variant with the maximum frequency, which often can be determined with higher certainty than the complete frequency distribution of the cultural variants present in the population.

To explore the effects of time averaging, we follow the approach suggested by Premo (2014). We determine time-averaged populations of cultural variants at time points t by randomly sampling N variants from a pool of variants generated by the nonaveraged populations produced by the simulation framework described above at the time points $t - i$, $i = 1, \ldots, a$. The effects of different strengths of time averaging can be investigated by varying the parameter a.

Statistical Inference

Our framework generates, among others, the variant with the highest frequency in averaged and nonaveraged populations at each time point conditioned on the considered cultural transmission modes. Based on this information, we can estimate the average time $t_{\max}$ a variant stays the most common variant in the population (see "Estimation of $t_{\max}$," below). To quantify the level of distinguishability of the considered modes based on an empirical estimate of $t_{\max}$, we calculate the overlap of the probability distributions of $t_{\max}$ for the transmission modes $x = v, h, o, u$. In more detail, the distribution of $t_{\max}$ conditioned on a transmission mode x indicates the range of time steps a variant stays the most common variant in a population that can be generated by mode x. Therefore, the size of the area of overlap, denoted by O_{xy}, between two distributions (see Figure 1 for an example) produced by the transmission modes x and y, respectively, reflects the certainty with which the corresponding transmission modes can be distinguished based on an estimate of $t_{\max}$.

If O_{xy} is sufficiently close to zero, then the transmission modes result mostly in different values of $t_{\max}$; consequently, distinguishability can be guaranteed (for details on the distinguishability criterion used, see Kandler et al. 2015). On the contrary, a value close to one indicates that the probability distributions are almost identical; therefore, the transmission modes cannot be distinguished on the basis of $t_{\max}$.

As already mentioned, we showed in Kandler et al. (2015) that, for high rates of change (e.g., for $P_{\text{within}} = 1$, which corresponds to on average five transmission events during an individual's lifetime

and $\mu = 0.1$), we can distinguish between vertical and horizontal transmission, vertical and unbiased transmission, unbiased and oblique transmission, and horizontal and oblique transmission based on t_{max}. In this situation the areas of overlap O_{xy} between the probability distributions produced by the different transmission modes are almost zero. Reducing the rate of change (e.g., reducing P_{within} and/or μ) results in larger areas of overlap O_{xy} and, consequently, less certainty in distinguishing between transmission modes.

Importantly, this conclusion was reached under the assumption that we have full knowledge about the most common variant at each point in the considered time interval. This, however, might only rarely be the case in historical case studies. Therefore, in the following we explore the temporal resolution of the time series that is needed in order to obtain inference results close to what is theoretically possible.

Distinguishability of Cultural Transmission Modes on the Basis of Incomplete Information

We assume that we have knowledge about the most common variant in the population at certain points in time but no information about the cultural composition of the population for the remaining time points (see Figure 2 for an illustration). Varying the number of sample points and the distance between the sample points allows us to determine the minimum requirements on the sample to still be able to distinguish between different transmission modes on the basis of an estimate of t_{max}. We focus only on the case where there is a high rate of change in the population, i.e., we assume $P_{within} = 1$ and $\mu = 0.1$. Otherwise, different transmission modes cannot be distinguished, even with perfect information (Kandler et al. 2015).

Estimation of t_{max}

We start our analysis by defining how the average time a variant stays the most common variant, t_{max}, is estimated based on incomplete temporal information about the cultural composition of the population. In the following we consider the time interval $1, \ldots, 200$. The time series $\{\nu(t)\}_{t=1,\ldots,200}$ records the variant with maximum frequency in the population at each time step t. It holds that $\nu(t) \in \{1, \ldots, 5\}$. Now a sample of size n with $n << 200$ is taken at the time points $t_S = \{t_1, \ldots, t_n\} \subset \{1, \ldots, 200\}$, and the observations $S = \{\nu(t_i)\}_{t_i \in t_S}$ describe the available information about the temporal dynamic of cultural change. Further, the distances between the sample points are denoted by $\Delta_i = t_{i+1} - t_i$, $i = 1, \ldots, n-1$. Based on the sample S we can determine the time points $\{t_{i_1}, \ldots, t_{i_{\bar{n}}}\} \subset t_S$ where the most common variant has changed. The variable $\bar{n}$ denotes the number of changes observed in the sample, and the average time a variant stays the most common in the population can then be estimated by

$$\hat{t}_{max} = \frac{1}{\bar{n}+1}\Big[t_{i_1} + (200 - t_{i_{\bar{n}}}) + \sum_{i=2}^{\bar{n}} (t_{i_i} - t_{i_{i-1}})\Big] = \frac{200}{\bar{n}+1} \quad (4)$$

Naturally, the accuracy of the estimate $\hat{t}_{max}$ is affected by the properties of the sample S, in particular by its size n and the distances $\Delta_{i=1,\ldots,n-1}$ between the sample points. To illustrate these influences, we determine the distributions of the estimate $\hat{t}_{max}$ for horizontal transmission and sample sizes $n = 5, 10, 20, 30, 40$ (Figure 3A). The distance between the sample points is chosen to be $\Delta_i = \Delta = 3$; that is, every three time points we obtain information about the most common variant in the population. The dashed line in Figure 3A shows the distribution of t_{max} based on the whole time series. We observe that the larger the sample size n, the tighter the distribution of $\hat{t}_{max}$. However, the "true" distribution of t_{max} is not well approximated even for relatively large n, pointing to the crucial importance of the distances $\Delta_i = \Delta$ between sample points. Figure 3B shows the distributions of the estimates $\hat{t}_{max}$ for horizontal transmission and $\Delta_i = \Delta = 1, 3, 5, 7, 10$. The sample size is assumed to be $n = 20$. Unsurprisingly, the

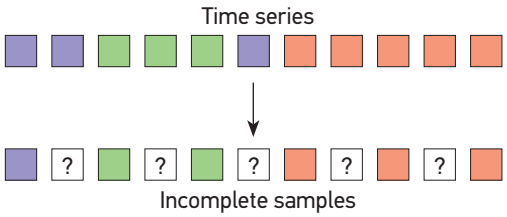

FIGURE 2. Incomplete available information: the most common variant in the population (represented by different colors) is known for only a subset of the time points in the considered interval.

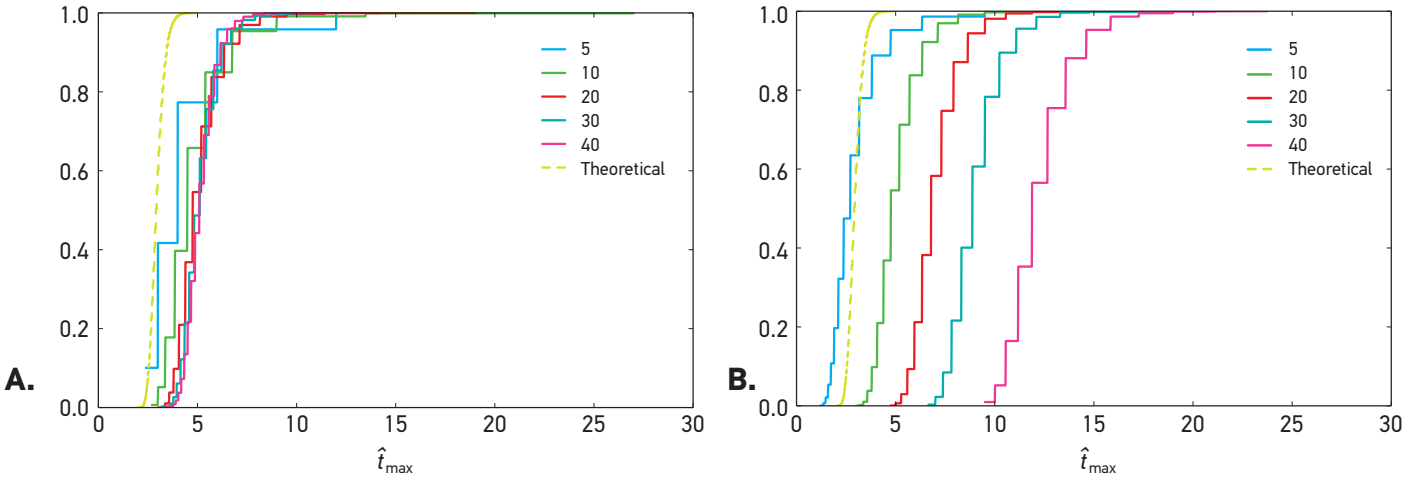

FIGURE 3. Estimates $\hat{t}_{max}$ for horizontal transmission: $n = 5$, 10, 20, 30, 40 and $\Delta_i = \Delta = 3$ (A) and $n = 20$ and $\Delta_i = \Delta = 1, 3, 5, 7, 10$. (B).

"true" distribution of t_{max} can only be well approximated for $\Delta = 1$. In this situation, an increase of the sample size n results in a more accurate approximation of t_{max}.

In the following we explore for which values of n and Δ_i we can obtain the theoretically possible distinguishability on the basis of incomplete information.

Hypothesis Test

Generally, to determine whether an estimate $\hat{t}_{max}$ derived from the empirical observations $\hat{S} = \{\hat{v}(t_i)\}$ at the time points $\hat{t}_S = \{\hat{t}_1, \ldots, \hat{t}_n\}$ is consistent with vertical, horizontal, oblique, or unbiased transmission, we need to determine the distributions $P(t^x_{max}|\hat{t}_S)$ of the average time a variant stays the most common variant in the population for each transmission mode $x \in \{v, h, o, u\}$. To do so we use the simulation framework and generate a time series $\{v^x(t)\}_{t=1,\ldots,200}$ conditioned on the transmission mode x with $x \in \{v, h, o, u\}$. We then determine the theoretical sample $S^x = \{v^x(t_i)\}_{i \in \hat{t}_S}$ based on the given sampling scheme $\hat{t}_S = \{\hat{t}_1, \ldots, \hat{t}_n\}$ and use Equation 4 to calculate the estimate of t_{max}. Repeating this process allows us to determine the distributions $P(t^x_{max}|\hat{t}_S)$ of t_{max} conditioned on the transmission mode $x \in \{v, h, o, u\}$ and the available sample points $\hat{t}_S = \{\hat{t}_1, \ldots, \hat{t}_n\}$. Now, if the estimate $\hat{t}_{max}$ is outside the $(1-\alpha) \times 100\%$ prediction interval of $P(t^x_{max}|\hat{t}_S)$, then we conclude that the transmission mode x could not have produced the observed data. Conversely, if the estimate falls within the prediction interval, we cannot rule out transmission mode x as possible underlying evolutionary force.

But how much information about the underlying transmission modes can be revealed by such a test? Even though we know that for $t_S = 1, \ldots, 200$ we can perfectly distinguish between certain transmission modes on the basis of an estimate of t_{max}, how much of this power is lost when considering only a sample at the time points $\hat{t}_S$?

To explore these questions we start by analyzing the size of the type II error of the suggested hypothesis test for different sampling schemes $t_S(n, \{\Delta_i\})$. (The type II error indicates the probability of failing to reject an incorrect null hypothesis.) We again generate data $\{v^y(t)\}_{t=1,\ldots,200}$ conditioned on the transmission mode $y \in \{v, h, o, u\}$, determine the sample S^y based on $t_S(n, \{\Delta_i\})$, and calculate the estimates $\hat{t}^y_{max}$ according to Equation 4. Lastly, we compare the estimate $\hat{t}^y_{max}$ with the $(1-\alpha) \times 100\%$ prediction interval of the distribution $P(t^x_{max}|t_S)$ of t_{max} under transmission mode x, denoted by $[a_x, b_x]$, and record whether the hypothesis

$\mathbb{H}$: Data was generated under transmission mode x

is rejected. Repeating this process gives us the probability $P_{xy}(t_S)$ of rejecting transmission mode x when the data were produced by transmission mode y. Analytically, the probability $P_{xy}(t_S)$ can be calculated by

$$\begin{aligned} P_{xy}(t_S) &= 1 - \int_{a_x}^{b_x} f_{t^y_{max}}(z|t_S)dz \\ &= 1 - F_{t^y_{max}}(a_x|t_S), \end{aligned} \tag{5}$$

where $f_{t^y_{max}}(\cdot|t_S)$ describes the density function of the statistic t_{max} under transmission mode y and

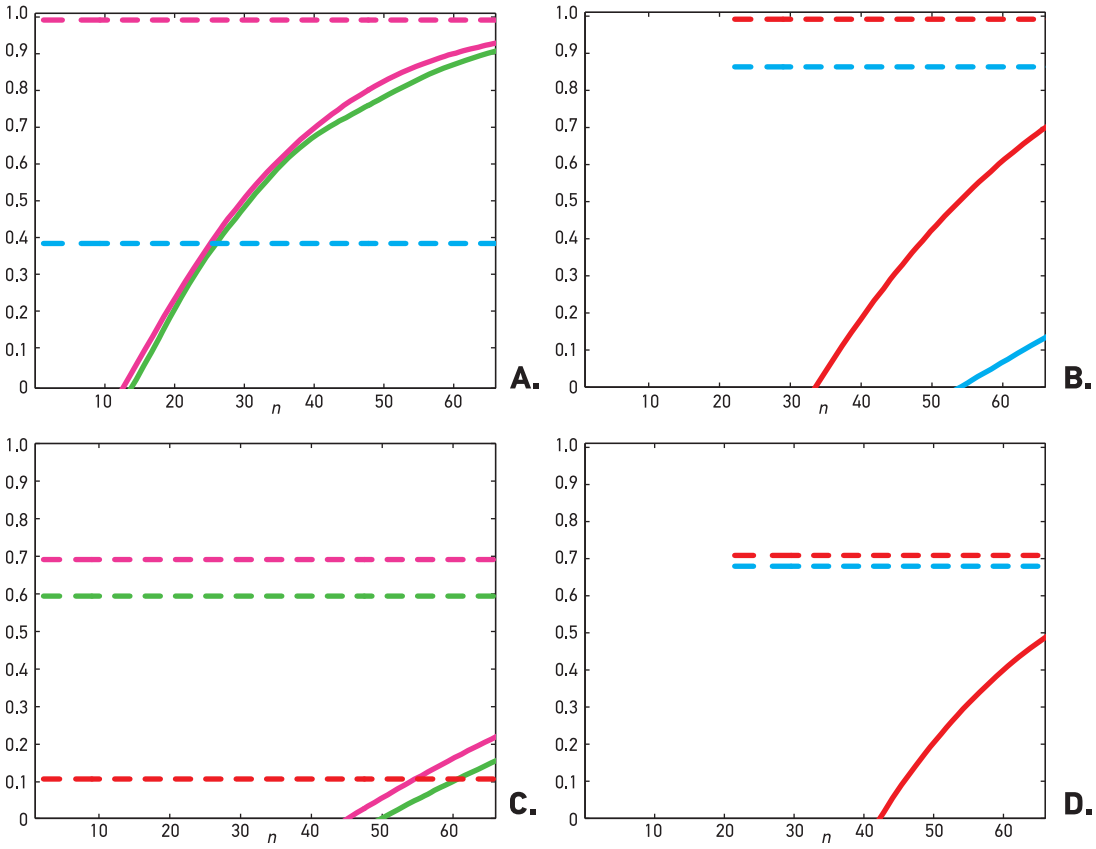

sample points t_S, and $F_{t^y_{\max}}(\cdot|t_S)$ denotes the corresponding distribution function. The type II error is given by $1 - P_{xy}(t_S)$.

Additionally, the knowledge of the theoretical distributions $P(t^x_{\max}|t_S)$ and $P(t^y_{\max}|t_S)$ allows us to quantify their area of overlap $O_{xy}(t_S)$ as a measure of distinguishability under incomplete information. If the area of overlap is small, then we can conclude that, on the basis of observations at the time points $t_S(n, \{\Delta_i\})$, the transmission modes x and y are distinguishable.

Results

In the following we analyze the rejection probability $P_{xy}(t_S)$ and the area of overlap $O_{xy}(t_S)$ with $x, y \in \{v, h, o, u\}$ for varying sample sizes n and distances between the time points $\{\Delta_i\}$ and explore which sequence of sample points $t_S(n, \{\Delta_i\})$ allows for reliable inference results.

Dependence on Sample Size *n*

Figure 4 shows the rejection probability $P_{xy}(t_S)$ as a function of the sample size n and $\Delta_i = \Delta = 3$. The observations $\{\nu^y(t_i)\}_{t_i \in t_S}$ are generated by vertical (Figure 4A), horizontal (Figure 4B), oblique (Figure 4C), and unbiased transmission (Figure 4D). The solid lines illustrate the rejection probabilities $P_{xy}(t_S)$ with $x \in \{v, h, o, u\}$, $x \neq y$, and the dashed lines describe the maximum rejection probability that can be obtained when observing every time point $t_s = [1, \ldots, 200]$.

Unsurprisingly, for small sample sizes n the probability of rejecting the "wrong" transmission mode is very small. The estimate $\hat{t}_{\max}$ is not precise enough to capture the differences in the temporal dynamic of cultural change. However, also for increased n we obtain rejection probabilities higher than 80% only for vertical and horizontal transmission and for vertical and unbiased transmission, implying that only these transmission modes can be distinguished reliably on the basis of incomplete information about the process of cultural change. Consequently even though it is theoretically

FIGURE 4. Rejection probability $P_{xy}(t_S)$ with $x, y \in \{v, h, o, u\}$ as a function of n and $\Delta_i = \Delta = 3$, and data generated according to vertical transmission (A), horizontal transmission (B), oblique transmission (C), or unbiased transmission (D). The red lines illustrate the rejection probability of the hypothesis of vertical transmission, the green lines of horizontal transmission, the blue lines of oblique transmission, and the magenta lines of unbiased transmission. The corresponding dashed lines show the highest possible rejection probability determined from observations at all time points $1, \ldots, 200$.

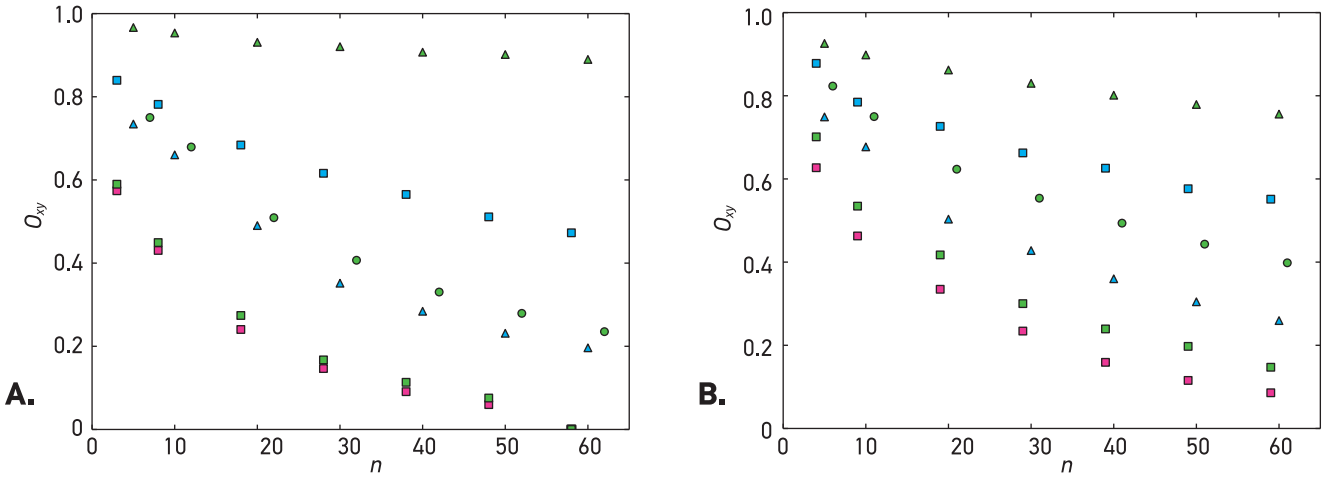

FIGURE 5. Area of overlap $O_{xy}(t_S)$ between the distributions $P(t^x_{\max}|t_S)$ and $P(t^y_{\max}|t_S)$ for x, $y \in \{v, h, o, u\}$ and $\Delta_i = \Delta = 3$ (A) and $\Delta_i = \Delta = 1$ (B). The squares show the difference between horizontal (green), oblique (blue), or random (magenta) transmission and vertical transmission; the triangles show the difference between oblique (blue) or horizontal (green) transmission and unbiased transmission; and the circles show the difference between horizontal transmission and oblique transmission.

possibly to distinguish between horizontal and oblique transmission and between unbiased and oblique transmission, we should not expect the same results when only incomplete information is available.

Figure 5A shows the area of overlap $O_{xy}(t_S)$ of the distributions $P(t^x_{\max}|t_S)$ and $P(t^y_{\max}|t_S)$ produced by the different transmission modes for n = 5, 10, 20, 30, 40, 50, 60 and $\Delta_i = \Delta = 3$. The squares show the difference between horizontal (green), oblique (blue), and unbiased (magenta) transmission and vertical transmission and therefore quantify the effect of cultural transmission occurring during the lifetime of an individual. The triangles show the difference between oblique (blue) or horizontal (green) transmission and unbiased transmission and therefore quantify the effect of restricting the set of possible transmission partners to partners within the same age group and to older partners, respectively. Lastly, the circles show the difference between horizontal transmission and oblique transmission. In agreement with Figure 4, we observe that the area of overlap $O_{xy}(t_S)$ decreases for increasing n; however, only vertical and horizontal transmission and vertical and unbiased transmission result in an area of overlap sufficiently small to ensure distinguishability. Figure 5B shows the areas of overlap $O_{xy}(t_S)$ for $\Delta_i = \Delta = 1$ and demonstrates that the ability to distinguish between transmission modes crucially depends on the chosen distance between the sample points, Δ_i. Interestingly, for the majority of combinations of x and y with $x \in \{v, h, o, u\}$, $x \neq y$, we obtain worse distinguishability results for $\Delta_i = \Delta = 1$ than for $\Delta_i = \Delta = 3$. This points to the fact that there exists an optimal distance between the observations, which we investigate in the next section.

Dependence on $\{\Delta_i\}$

We saw in the last section that variations in the distance Δ_i between the sample points t_i and t_{i+1} greatly influence the distinguishability results. In the following, we present the results of the analysis based on constant distance between the sample points (i.e., $\Delta_i = \Delta$), but we also carried out the same analysis with exponentially distributed distances (i.e., $t_{i+1} - t_i \sim \exp(1/\Delta)$ for $\Delta \geq 1$) and obtained very similar results (see Figure 7).

Figure 6 shows the rejection probability $P_{xy}(t_S)$ with $x, y \in \{v, h, o, u\}$, $x \neq y$, in dependence of Δ. The sample size is assumed to be n = 20. Similarly to Figure 4, observations $\{v^y(t_i)\}_{t_i \in t_S}$ are generated by vertical (Figure 6A), horizontal (Figure 6B), oblique (Figure 6C), and unbiased transmission (Figure 6D). The solid lines illustrate the rejection probabilities $P_{xy}(t_S)$ with $x \in \{v, h, o, u\}$, $x \neq y$, and the dashed lines describe the maximum rejection probability that can be obtained when observing every time point $t_s = [1, \ldots, 200]$. First, we observe that for each pair of transmission modes (x, y) there exists a Δ that produces the maximum rejection probability $P_{xy}(t_S)$. As already indicated by Figure 5, those maximum rejection probabilities are often not obtained for Δ = 1. Intermediate values of Δ ranging from 2 to 5 provide the best distinguishability results for the assumed situations of cultural change (N = 100, Δ = 0.1, P_{within} = 1). Consequently,

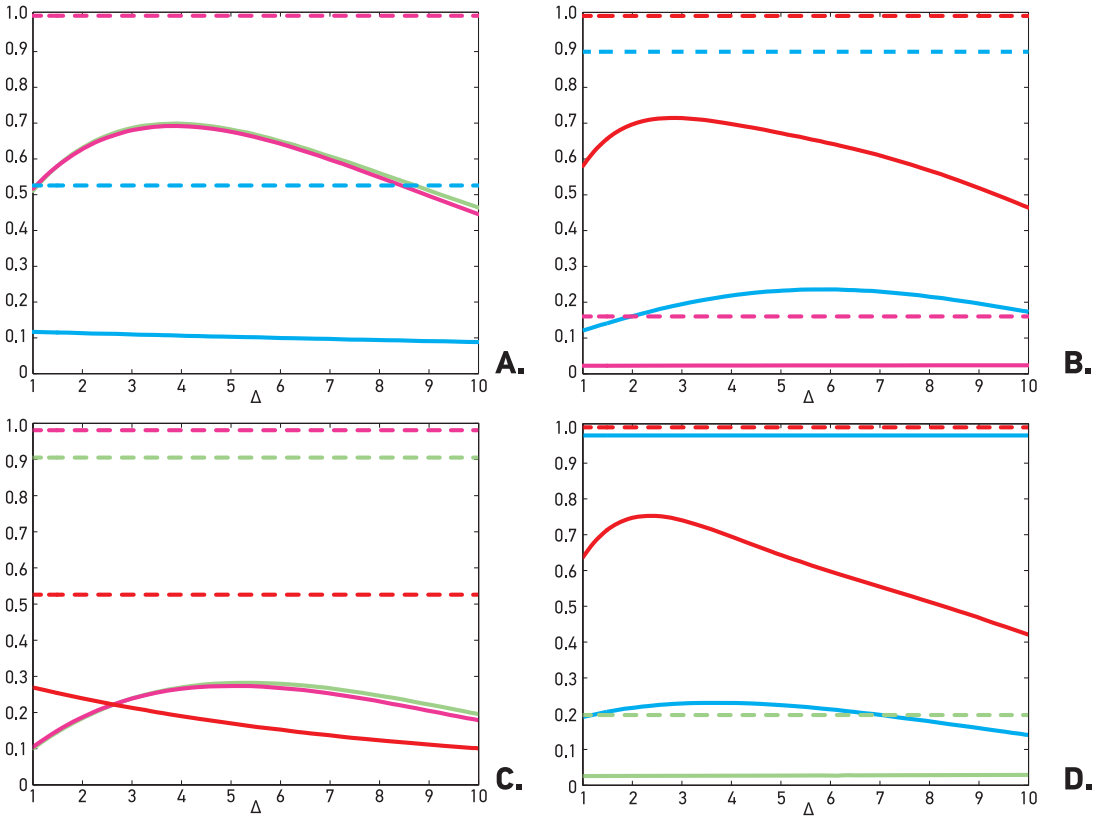

FIGURE 6. Rejection probability $P_{xy}(t_S)$ with $x, y \in \{v, h, o, u\}$ as a function of $\Delta_i = \Delta$, $n = 20$ and data generated according to vertical transmission (A), horizontal transmission (B), oblique transmission (C), and unbiased transmission (D). The red lines illustrate the rejection probability of the hypothesis of vertical transmission; the green lines, of horizontal transmission; the blue lines, of oblique transmission; and the magenta lines, of unbiased transmission. The corresponding dashed lines show the highest possible rejection probability determined from observations at all time points $t = 1, \ldots, 200$.

the sampling scheme that provides the best inference result is the one that produces distributions $P(t^x_{\max}|t_S)$ and $P(t^y_{\max}|t_S)$ as different as possible and not necessarily the most accurate estimation of $t_{\max}$. Further, we observe that the rejection probabilities $P_{xy}(t_S)$ decrease for large values of Δ, indicating that samples taken at too distant time points do not carry much information about the underlying process; the time series becomes more and more uncorrelated.

Figure 7 shows the area of overlap $O_{xy}(t_S)$ of the distributions $P(t^x_{\max}|t_S)$ and $P(t^y_{\max}|t_S)$ produced by the different transmission modes for $\Delta_i = \Delta = 1, 3, 5, 7, 10$ and $n = 20$. We observe a similar behavior: almost every combination of x and y with $x, y \in \{v, h, o, u\}, x \neq y$, requires a different value of Δ to achieve the smallest area of overlap.

Effects of Time Averaging

To explore the effects of time averaging we determine (time-averaged) populations of cultural variants at each time point t by randomly sampling N variants from a pool of variants generated by the (nonaveraged) populations produced by the simulation framework at the time points $t - i$, $i = 1, \ldots, a$. Thus, the time series $\{\nu_{\text{average}}(t)\}_{t=a+1,\ldots,200}$ now records the variant with maximum frequency in the averaged population, whereby averaging occurred over the last a time steps.

Figure 8 shows the results of the distinguishability analysis for $\Delta_i = \Delta = 1, 3, 5, 7, 9$; $n = 20$, and averaging windows of size $a = 5$ and $a = 10$. It is obvious that the areas of overlap $O_{xy}(t_{\text{average},S})$ of the distributions $P(t^x_{\max}|t_{\text{average},S})$ and $P(t^y_{\max}|t_{\text{average},S})$ produced by the different transmission modes are increased compared with the situation without time averaging (see Figure 7). It holds that the larger the averaging window a, the larger the area of overlap and therefore the smaller the certainty with which two transmission modes can be distinguished. However, even for $a = 10$ the probability distributions $P(t^x_{\max}|t_{\text{average},S})$ and $P(t^y_{\max}|t_{\text{average},S})$ are not identical. In the best situation, we obtain an overlap of roughly 45%, indicating that either smaller or larger values of $t_{\max}$ can be reached only by one transmission mode or the other.

To summarize, time averaging dilutes the detectable signal of cultural transmission modes in population-level data but does not remove it completely.

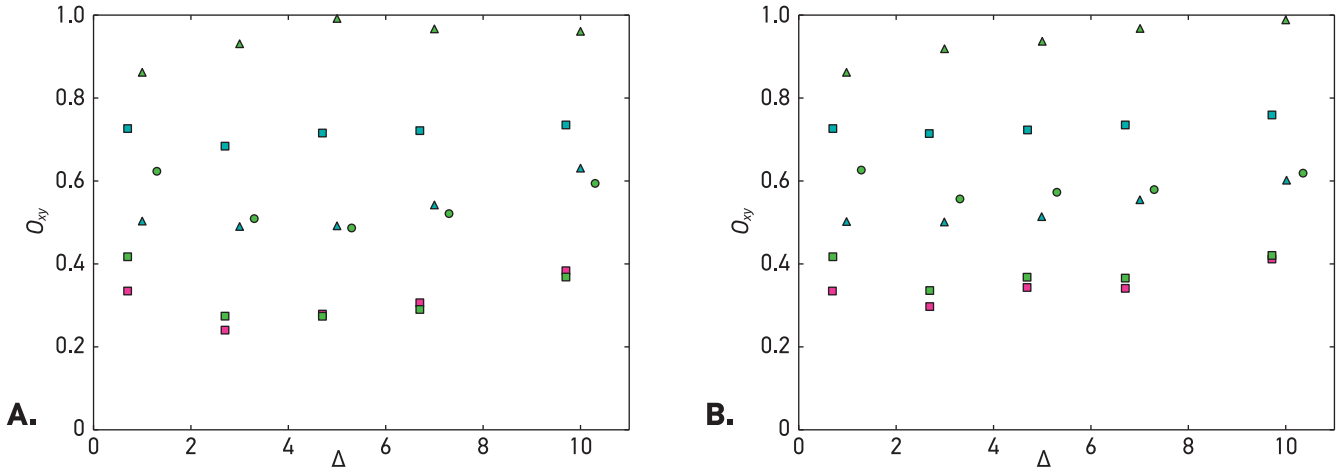

FIGURE 7. Area of overlap $O_{xy}(t_s)$ between the distributions $P(t^x_{max}|t_S)$ and $P(t^y_{max}|t_S)$ for x, $y \in \{v, h, o, u\}$, $n = 20$, $\Delta_i = \Delta = 1$, 3, 5, 7, 10 (A) $t_{i+1} - t_i \sim \exp(1/\Delta)$ for $\Delta \geq 1$ (B). Colors and shapes correspond to those in Figure 5.

Conclusion

In this article we used a simulation framework to explore whether vertical, horizontal, oblique, and unbiased transmission can be distinguished on the basis of incomplete information about temporal change in the cultural composition of the population. We built our analysis on insights gained in a previous study (Kandler et al. 2015), which showed that the temporal dynamic of cultural change carries a stronger signature of the underlying transmission modes than the knowledge of the whole cultural composition of the population a specific point in time expressed by, for example, the level of cultural diversity. To describe the temporal dynamic of cultural change, we determined the average time a variant stays the most common variant in the population, denoted by t_{max}. Using the simulation framework we generated the distributions t^x_{max}, $x \in \{v, h, o, u\}$, of t_{max} conditioned on the considered transmission modes x.

These distributions illustrate the values of t_{max} that are possible under x, and therefore the overlap O_{xy} between two distributions $P(t^x_{max})$ and $P(t^y_{max})$ provides a measure of the certainty with which two transmission modes x and y can be distinguished. Only if these two distributions are sufficiently different can distinguishability be guaranteed. We showed in Kandler et al. (2015) that for high rates of change (i.e., individuals have frequent opportunities to engage in cultural transmission during their lifetime) the temporal dynamic of cultural change is very different between vertical and horizontal transmission, vertical and oblique transmission, vertical and unbiased transmission, unbiased and oblique transmission, and horizontal and oblique transmission and conclude that it is possible to perfectly distinguish between these transmission

FIGURE 8. Area of overlap $O_{xy}(t_s)$ between the distributions $P(t^x_{max}|t_{average,\,S})$ and $P(t^y_{max}|t_{average,\,S})$ for x, $y \in \{v, h, o, u\}$, $n = 20$, $\Delta_i = \Delta = 1$, 3, 5, 7, 9, $\alpha = 5$ (A) and $\alpha = 10$ (B). Colors and shapes correspond to those in Figure 5.

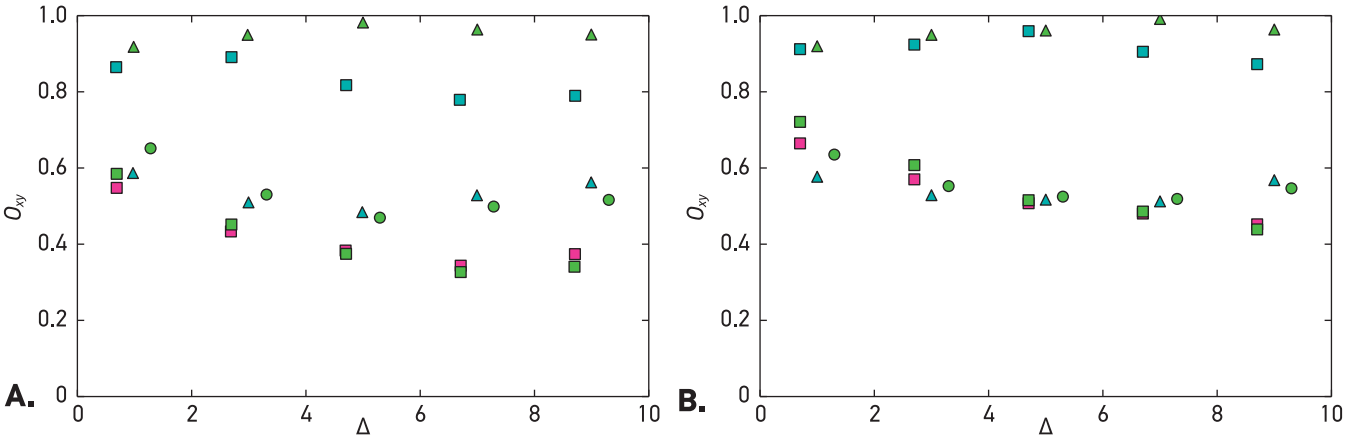

modes on the basis of the statistic t_{max}. Reducing the rate of change results in probability distributions with a greater overlap and consequently less certainty in distinguishing between transmission modes based on an estimate of t_{max}.

Crucially, in Kandler et al. (2015) we reached this conclusion under the assumption that we have full knowledge about the most common variant at every point in the considered time interval. This, however, might only rarely be the case, especially in historical case studies. Therefore, in this article we explored whether the obtained distinguishability results hold for situations with incomplete temporal information about the most common variant in the population. We assumed that samples are taken at the time points $t_s = \{t_1, \ldots, t_n\}$ and investigated the influence of the sample size n and the distance between the sample points Δ on the ability to infer underlying transmission modes from population-level data.

The average time a variant stays the most common variant in the population is determined by Equation 4. Naturally, those estimates are precise only if sufficiently many observations at consecutive time steps (i.e., $\Delta = 1$) are available. However, the aim of this analysis was *not* to obtain the most precise estimate of t_{max} but to determine the sampling scheme $t_s = t_s(n, \{\Delta_i\})$ that produces distributions of t_{max} that are as different as possible under the considered transmission modes. For that, n should be chosen as high as possible. But as transmission modes usually operate on different time scales, we found that different pairs (x,y) of transmission modes require different values of Δ to achieve the smallest possible area of overlap $O_{xy}(t_s)$ for a given n (see Figure 7). Consequently, we need to determine the value of Δ that provides an acceptable statistical power to distinguish between all considered transmission modes. We suggest that simulation frameworks, similar to the one considered here, that capture the main dynamics of the analyzed case study could help determine the properties of the sampling scheme that produce the highest possible power to distinguish between transmission modes. In situations where data have been already collected at time points t_s, a simulation framework can explore whether it is theoretically possible to distinguish between transmission modes on the basis of a single estimate of t_{max}. Additionally, the simulation framework generates for each sampling scheme and transmission mode x the distribution $P(t^x_{max}|t_S)$ of t_{max} allowing for statistical hypothesis testing.

In summary, even though it is possible to perfectly distinguish between certain transmission modes on the basis of complete information about the most common variant in the population, we should not expect the same result if only a sample taken at the time points t_s is available (see, e.g., Figures 5 and 7). In situations of incomplete information, the level of distinguishability depends crucially on the properties of the sample. We have shown that the distance Δ between the time points at which the samples are taken has a strong influence on the amount of information about the underlying transmission mode that can be inferred from population-level data. If Δ is too large, that is, if the sample points are too distant from each other, then an increase in the sample size n will not improve the results greatly. If the observed population-level data are a product of time-averaging processes, we should expect even less certainty in distinguishing between different cultural transmission modes. However, the detectable signal of transmission modes in population-level data is not removed completely.

Consequently, it is unlikely that sparse population-level data such as knowledge about the most common cultural variant in the population at certain points in time will allow for *unique* inference of the cultural transmission mode that produced the data. Different transmission modes will be consistent with the data. However, this conclusion does not render mathematical modeling meaningless. To the contrary, it is important, first, to understand the theoretical limits to statistical inference procedures and therefore to understand which kinds of questions can be answered with which kinds of data. Second, the analysis of population level data might help exclude transmission modes that could *not* have produced the observed data and in this way lead to a reduction of the pool of potential hypotheses. Subsequently, different lines of evidence might be used to reduce this pool even further.

ACKNOWLEDGMENTS

The authors thank Tanmoy Bhattacharya for insightful discussions on this topic. Further, we thank three anonymous reviewers for their constructive comments, which helped in improving the manuscript. This research was supported by a National Science Foundation Early Concept Grants for Exploratory Research grant (EAGER 1249146, "Linking Pattern and Process in Cultural Evolution," to Laura Fortunato and A.K.).

Received 31 December 2014; revision accepted for publication 19 June 2015.

LITERATURE CITED

Baum, W. M., P. J. Richerson, C. M. Efferson et al. 2004. Cultural evolution in laboratory microsocieties including traditions of rule giving and rule following. *Evol. Hum. Behav.* 25:305–326.

Bentley, R. A., M. W. Hahn, and S. J. Shennan. 2004. Random drift and culture change. *Proc. Roy. Soc. B.* 271:1,443–1,450.

Bentley, R. A., C. Lipo, H. A. Herzog et al. 2007. Regular rates of popular culture change reflect random copying. *Evol. Hum. Behav.* 28:151–158.

Boyd, R., and P. J. Richerson. 1985. *Culture and the Evolutionary Process.* Chicago: University of Chicago Press.

Beheim, A. B., C. Thigpen, and R. McElreath. 2014. Strategic social learning and the population dynamics of human behavior: The game of Go. *Evol. Hum. Behav.* 35:351–357.

Cavalli-Sforza, L., and M. W. Feldman. 1981. *Cultural Transmission and Evolution: A Quantitative Approach.* Princeton, NJ: Princeton University Press.

Eerkens, J. W., R. L. Bettinger, and R. McElreath. 2005. Cultural transmission, phylogenetics and the archaeological record. In *Mapping Our Ancestors*, C. P. Lipo, M. J. O'Brian, M. Collard, and J. Shennan, eds. New York: Transaction, 316–334.

Evans, T. S., and A. Giometto. 2011. Turnover rate of popularity charts in neutral models. Preprint. arXiv:1105.4044 [physics.soc-ph].

Henrich, J. 2001. Cultural transmission and the diffusion of innovations: Adoption dynamic indicate that biased cultural transmission is the predominant force in behavioural change. *Am. Anthropol.* 103:992–1,013.

Henrich, J., and J. Broesch. 2011. On the nature of cultural transmission networks: Evidence from Fijian villages for adaptive learning biases. *Philos. Trans. R. Soc. Lond. B Biol. Sci.* 366:1,139–1,148.

Kandler, A., B. Wilder, and L. Fortunato. 2015. Inferring the process of cultural evolution from population-level patterns. Unpublished manuscript.

Kidwell, S. M., and A. K. Behrensmeyer. 1993. *Taphonomic Approaches to Time Resolution in fossil assemblages.* Short Courses in Paleonthology 6. Knoxville, TN: Paleontology Society.

Kowalewski, M. 1996. Time-averaging, overcompleteness, and the geological record. *J. Geol.* 104:317–326.

Laland, K. N. 2004. Social learning strategies. *Learn. Behav.* 32:4–14.

Madsen, M. 2012. Unbiased cultural transmission in time-averaged archaeological assemblages. Preprint. arXiv:1204.2043 [physics.soc-ph].

Mesoudi, A., and M. J. O'Brien. 2008. The cultural transmission of great basin projectile-point technology I: An experimental simulation. *Am. Antiq.* 73:3–28.

Morgan, T. J. H., L. Rendell, M. Ehn et al. 2012. The evolutionary basis of human social learning. *Proc. Roy. Soc. B.* 279:653–662.

Porčić, M. 2014. Exploring the effects of assemblage accumulation on diversity and innovation rate estimates in neutral, conformist, and anti-conformist models of cultural transmission. *J. Archaeol. Method Theory*, doi:10.1007/s10816-014-9217-8.

Premo, L. S. 2014. Cultural transmission and diversity in time-averaged assemblages. *Curr. Anthropol.* 55:105–114.

Rendell, L., R. Boyd, D. Cowden et al. 2010. Why copy others? Insights from the social learning strategies tournament. *Science* 328:208–213.

Rendell, L., L. Fogarty, W. J. E. Hoppitt et al. 2011. Cognitive culture: theoretical and empirical insights into social learning strategies. *Trends Cogn. Sci.* 15:68–76.

Shennan, S. 2011. Descent with modification and the archaeological record. *Philos. Trans. R. Soc. Lond. B Biol. Sci.* 366:1,070–1,079.